Supporting information:

T cell activation is determined by the number of presented antigens

*Janosch Deeg[1,2], Markus Axmann[1,2], Jovana Matic[1,2], Anastasia Liapis[3], David Depoil[3], Jehan Afrose[3], Silvia Curado[3], Michael L. Dustin[3,4] and Joachim P. Spatz[1,2]**

[1]Department of New Materials and Biosystems, Max Planck Institute for Intelligent Systems, Heisenbergstraße 3, D-70569 Stuttgart, Germany

[2]Department of Biophysical Chemistry, University of Heidelberg, INF 253, D-69120 Heidelberg, Germany

[3]Skirball Institute of Biomolecular Medicine and Department of Pathology, New York University School of Medicine, New York, NY 10016

[4]Kennedy Institute of Rheumatology, Nuffield Department of Orthopedics, Rheumatology and Musculoskeletal Sciences, University of Oxford, Oxford, OX37FY, United Kingdom

*Corresponding author: spatz@is.mpg.de

Experimental Details:

Block-Copolymer Micelle Nanolithography: In order to yield 30-300 nm spaced nano-patterns $AuCl_4$-containing micelle solutions of various polystrene-block-poly(2-vinylpyridine) (PS-b-P2 VP) diblock copolymers (Polymer Source Inc., Dorval, Canada) were prepared as previously described (R. Glass 2003, Spatz 2000). Piranha-cleaned glass slides were retracted from the micelle solution described above by a custom-made device at a defined speed. Upon drying, substrates were treated with hydrogen plasma (45 min., 600 W, 0.3 mbar, TePla PS 210, Wettenberg, Germany) (see also Fig. S1a,b).

Photolithography: Substrates with Au nanoparticle arrays were spin-coated with a 1.1-1.3 µm thick layer of SU-8-2 negative resist (Micro Resist Technology GmbH, Berlin, Germany). Soft-baking was performed according to the manufacturer's instructions and the microstructure was transferred to the resist layer by illumination through a chromium mask with UV light of a HBO 350 mercury lamp at a dose of 50 mJ/cm^2. After post-exposure baking the structure was developed in the recommended developer solution (MR-Dev600, Micro Resist Technology GmbH, Berlin, Germany). Unprotected particles were detached by sonication for two min. in an aqueous solution of 1% cysteamine. Eventually, the highly cross-linked resist was removed by hydrogen plasma treatment (150 min., 150 W; 0.4 mbar, TePla 100-E, Wettenberg, Germany) (see also Fig. S1c).

Structure analysis: Structure dimensions were analyzed by scanning electron micrographs using ImageJ (http://rsbweb.nih.gov/ij/) and a custom-made plug-in (kindly provided by Philipp Girard) comparing the generated pattern to an ideal hexagonal pattern. Particle distances and densities of the quasi-hexagonally ordered patterns were calculated and respective errors were obtained by Gaussian error propagation. The SEM pictures were performed using a Zeiss LEO 1530 (ZeissSMT, Oberkochen, Germany) with acceleration voltages of approximately 5 keV and working distances between 5 and 10 mm.

Purification of IE^k-MCC-Cys: IE^k-MCC-Cys-producing S2 cells were grown in Sf-900 IIITMSFM medium (Invitrogen) at 27°C, 90 rpm shaker incubator, and induced for three days at 20 million/ml with 0.5 mM copper (II) sulfate ($CuSO_4$). The supernatant was collected by centrifuging the cells down at 3000 rpm for 10 min. and filtered through 0.22 µm Millipore Stericup filters (Millipore). 1mM EDTA and 0.05% azide was added to the supernatant to prevent protein degradation. The purification of IE^k-MCC-Cys was carried out following standard cobalt-column affinity purification at 4°C. His Pur™ resin (Thermo scientific) was washed with equilibration buffer (50 mM sodium phosphate, 300 mM sodium chloride, 10 mM imidazole, pH 7.4) and the equilibrated resin was slowly stirred overnight with the filtered supernatant at 4°C. The resin was then transferred into an empty column cartridge (Thermo scientific) and washed with five resin-bed volumes of equilibration buffer for three times. The protein was eluted with elution buffer (50 mM

sodium phosphate, 300 mM sodium chloride, 150 mM imidazole, pH 7.4). The absorbance of the eluted fractions was measured at 280 nm and run in SDS-PAGE gel for protein detection. All cobalt fractions containing IE^k-MCC-Cys (molecular weight 65 kDa) were pooled together and further purified through a gel filtration column, HiLoad 16/600 Superdex 200 prep grade (GE healthcare) in AKTA xpress.

Bio-functionalization: Substrates were rendered hydrophilic by a reactive hydrogen plasma (6 min., 150 W, 0.4 mbar, TePla 100-E, Wettenberg, Germany) before they were placed into a custom-made glass rack and transferred into a clean glass flask containing a 1 mM solution of the linear poly-(ethylene glycol) mPEG2000-urea (CH_3-O-(CH_2-CH_2-O)$_{43}$-NH-CdO-NH-CH_2-CH_2-CH_2-Si(OEt)$_3$) in dry toluene (Merck) and 0,05% triethylamine (99,5%, Sigma Aldrich). Samples were kept at 80°C under nitrogen atmosphere for at least 12 hours (covalent coupling of PEG). Slides were then removed from the flask and sonicated 3 times for 5 min. in ethylacetate (p. A., Merck) and 3 times in methanol (p. A., Sigma Aldrich) and dried. The glass slides were immediately placed upon a droplet of NTA (1 mM) in pure ethanol (Sigma-Aldrich) and incubated for at least 1 hour at 4°C, then rinsed with pure ethanol and dried with pure nitrogen. The glass bottoms of 8 well Lab-Tek Chambers (Sigma-Aldrich) were removed and replaced by the bio-functionalized surfaces. The chambers were incubated for 20 min. in a 100 mM aqueous solution of nickel-chloride, rinsed with phosphate buffered saline (PBS), followed by an incubation with His-tagged pMHC (5 µg/ml) over night at 4°C. Before seeding the cells, the samples were intensively rinsed with PBS. Additionally, several types of control surfaces were used. As positive controls, appropriate Lab-Tek chambered

glass slides were incubated with pMHC or entirely Au-coated glass slides were biofunctionalized with NTA-Ni and His-tagged pMHC as described above. Negative controls consisted of either glass slides without Au particles (PEG surfaces) processed the same way as the structured surfaces, or appropriate Lab-Tek chambered glass slides without any treatment.

Quantification of pMHC molecules per particle:

Samples were prepared, processed and evaluated as described in the fabrication, bio-functionalization and image analysis section. The background was bio-inert due to a covalently-bound PEG layer and particles served as anchor for the pMHC, IE^k-2xHis_6-MCC-Atto655 attached via NTA-Ni. The pMHC concentration was 5 µg/ml for bulk measurements and was reduced by a factor of 100 to determine the single molecule signal. All experiments were performed on a modified Axiovert 200M epi-fluorescence microscope (Zeiss, Germany) at 37 °C (Incubator XL S1, Heating Stage P Lab-Tek S1, Objective Heater S1, Zeiss). For excitation of the fluorophore, a diode laser (iBeam smart 640, Toptica, Germany), which was directly modulated in time, was employed. The laser light was coupled into the microscope using a custom-built free-beam-path optical system. The field of sample excitation was limited using a rectangular aperture in the optical pathway. The sample was excited via a 100x, NA=1.46 Apochromat objective (Zeiss) for an illumination time of t_{ill}=1 ms at 640 nm with an intensity of 5 kW/cm² (measured on the sample plane). The excitation wavelength was separated from the fluorescence using a dichroic mirror (z405/515/647/1064rpc, Chroma, USA). The fluorescence itself was

104 split in the detection pathway using the Optosplit-II-device (Cairn Research, UK) and a
105 custom filter combination (HC Beamsplitter 662 imaging, Brightline HC 685/40,
106 Semrock). Images were recorded on a back-illuminated, liquid-cooled EMCDD camera
107 (iXon Ultra 897, Andor, UK) operated at 17 MHz readout speed with a varying EM gain.
108 A self-written software (Labview, National Instruments, USA) generated the timing
109 protocol for the diode lasers/ camera and recorded the images.

110 Images were analyzed using self-written algorithms in Matlab (Mathworks, USA). The
111 position of individual diffraction-limited fluorescence signals, as well as its width σ,
112 intensity and level of background noise, was determined using a Bayesian estimation
113 algorithm. Bayes Rule gives the probability $p(D/H)$ of an experimentally-obtained
114 intensity distribution D for a hypothesis H as $p(D/H) = p(H/D) \cdot p(D)/p(H)$, H in this
115 study, being a Gaussian intensity distribution with the 5 parameters x-Position, y-Position,
116 width, intensity and noise level (standard deviation of the background signal). Given that
117 $p(D)$ is independent of the hypothesis-parameters and equal to 1, the equation can be
118 simplified to $p(D/H) = p(H/D)/p(H)$. The algorithm determines the maximum
119 probability $p(H/D)$ by variation of the hypothesis-parameters within the prescriptive,
120 theoretical limits for individual and diffraction-limited fluorescence signals. Depending
121 on the actual hypothesis-parameters, the expectancy value of the intensity for each pixel
122 is estimated through the underlying Poisson statistics. The probability $p(D/H)$ for a
123 whole 5 x 5 pixel sub-image area was calculated as the product of the 25 individual pixel
124 probabilities (for background noise level a 7 x 7 pixel area was used). After localization
125 of the maximum intensity value in the sub-image, a recursive, and for each parameter
126 independent (because of the convex function characteristics of the intensity), an iterative

line search method was used in order to determine the values of all parameters for the maximized probability value.

In order to determine the average number of pMHC molecules per Au-nanoparticle the fluorescence intensity of areas sized 110 μm^2 was determined and compared with the average intensity value of one single pMHC molecule. The resulting number of pMHC molecules per area could be related to the amount of nanoparticles within the measured area. After correction for the background signal obtained from a sample incubated with unlabeled protein, this value was divided by the calculated average single molecule intensity ($N > 300$). Because every parameter, such as incubation time, concentration of protein, washing steps, influences the signal intensity, a strict protocol was followed (see above) and chambers used for cell experiments were used. Fig. S2 shows the occupational rate of pMHC molecule per Au particle for surfaces with particle spacings between 100-150 nm. This particular distance range was chosen as this was shown to be the critical regime regarding T cell stimulation and allowed for the determination of the corresponding critical density. It should be noted that the fluorescent signal from a sample incubated with unlabeled protein did not differ from a sample without any protein. A negative control without Au-nanoparticles or without the linker molecule yielded similar negligible results. After correction for the labeling rate of the protein itself (here 60%), the resulting protein density value was compared with the Au-nanoparticle intensity to calculate the mean protein/particle ratio, which was found to be 1.6 ± 0.4 molecules per particle. In order to show specificity of binding within the same surface, particle islands separated by empty areas were imaged (see main text).

Preparation of cells:

AND TCR transgenic mice were purchased from Jackson Laboratories (Bar Harbor, ME) and were crossed to B10.Cg-Tg (TcrAND) 53Hed/J (B10.AND). AND mice are alpha/beta TCR transgenic mice produced using the alpha and beta chain genes that encode a receptor specific for pigeon cytochrome c in association with IE^k class II MHC molecules. The TCR expressed in these mice is composed of alpha and beta chains derived from the cytochrome-c specific T-cell clones AN6.2 and 5C.c7, respectively. This TCR is termed "AND" (for references see main text). All mice were housed in specific pathogen-free conditions and cared for in accordance with the protocol approved by Institutional and Animal Care and Use Committee. Experiments were performed on F1 progenies between 8 and 12 weeks of age. AND TCR Tg splenocytes cells were activated in DMEM (Invitrogen) with 10% fetal bovine serum (FBS) (Hyclone) using 1 μM MCC peptide (MCC88-103). At 48 hours, cells were washed twice in complete medium and were plated at $1x10^6$ cells/ml with 50 U/ml of IL-2. The cells were replenished with fresh media and IL-2 every two days. After six days cells were deep-frozen and shipped to the laboratory where experiments were performed.

Cells were stored in liquid nitrogen and thawed approximately 24 hours prior to being seeded on nanopatterned surfaces. The cells were cultured in the appropriate liquid medium (RPMI 1640 with phenol red and glutamine, Invitrogen) supplemented with 10% FBS (Invitrogen) and 1% penicillin-streptomycin in cell culture flasks.

Activation experiments:

172 Cell suspensions were taken out of the cell culture flask, centrifuged, re-suspended in
173 complete medium (details above) to achieve a cell density of 500 cells/µl. The cell
174 density, which included a fraction of dead cells, was determined using trypan blue and a
175 Neubauer Hemocytometer. 300 µl of cell-suspension ($1.5x10^5$ cells) were added to each
176 chamber presenting a bio-functionalized glass surfaces as bottom.

177 Alpha tubulin staining: 45 min. after the cells had been seeded on the surface and kept
178 at 37 °C and 5% CO_2, they were fixed with 4% paraformaldehyde (PFA) at 37 °C for 10
179 min. before being permeabilized with ice-cold methanol for 1 min. and washed three
180 times with PBS and 2% bovine serum albumin (BSA). The surfaces were then incubated
181 with monoclonal anti-beta tubulin Cy-3 labeled antibody (Sigma-Aldrich) at a
182 concentration of 10 µg/ml in PBS containing 2% BSA. The chambers were rinsed with
183 PBS containing 2% BSA. Stained cells were imaged with an inverted fluorescence
184 microscope (Olympus IX71, HBO lamp, Sony CCD Camera, Deltavision system) using
185 appropriate filters and a 60-fold objective (Olympus).

186 Adhesion experiments: 45 ± 15 min. after the cells had been in contact with the surface
187 at 37 °C and 5% CO_2, cells were imaged with a custom-made reflection interference
188 contrast microscope (RICM). Images were taken randomly and the fraction of adherent
189 cells was calculated by manually counting adherent cells and non-adherent cells ($n > 100$
190 adherent cells for each data point). The fraction of dead cells (usually 30-40%), which
191 was determined before seeding, was subtracted from the number of non-adherent cells.
192 The contact area was determined using ImageJ by manually outlining the edge of cells (n
193 > 100 for each data point, except for cells plated on particle distances above 150 nm;
194 where $n > 15$ because of very low adhesion).

ELISA (IL-2 secretion): 200 μl of supernatant were taken out of the chambers after 24 hours of cell culture at 37 °C and 5% CO_2 and were used to determine the IL-2 concentration within the medium with a high sensitivity ELISA analysis Kit from eBioscience (Mouse IL-2 ELISA Ready-SET-Go!®).

Error Discussion:

Determination of contact area:

The choice of 45 min. as measure point for T cell activation was based on practical experience. In theory T cells start to establish contact with the APC surface immediately after detection of antigen by the TCR. This cell contact can be formed within a short time period, and indeed it was observed in this study that some cells could reach their maximal size 2-10 min. after encountering the antigen. However, cells migrating on the surface before starting to spread could also be observed. Moreover, after being seeded, cells have to sink down to the bottom of the culture surface to be in contact with the surface. Once attached the majority of cells was found to remain adherent for up to two hours and then to migrate or show a smaller spreading extension. These time frames correlate well with the dynamics of IS formation, which is reported to start initially after antigen detection and to last up to two hours. Given these experimental observations and theoretical background, we found it reasonable to start measurements not before 30 min. after seeding and continued to acquire images for 30 min. It is possible that some cells might have shown a larger spreading area before images were taken, while others may had not

yet reached their maximal size at the time point of image acquisition. Furthermore, it is possible that some cells were still migrating and not adhesive and even migrating again after having already spread. However, for this study, it is not crucial, nor possible, to measure exactly the peak sizes of the spreading area. For mean values at a certain time point the different stages of spreading of individual cells averaged out. Moreover, we found the spreading area by itself not to be sufficiently indicative of T cell stimulation since the spreading area did not decrease significantly when nanoparticles were widely spaced, unlike other parameters tested that showed a clear correlation.

Quantification of the percentage of adherent cells: The number of spread cells was determined manually by counting the number of adherent and non-adherent cells in images randomly acquired. A software-based automated detection routine failed to determine the number of spread cells because of the difficulty to distinguish between non-adherent and adherent cells. While adherent cells (correspondent to black patches) can be detected it is very challenging to detect non-adherent cells.

Nevertheless, the manually collected data of number of adherent cells was included since the cellular contact area criteria alone was not enough to distinguish between stimulating/ non-stimulating substrates. The reason is due to the fact that those cells that spread, of course, reach a certain minimal spreading area. However, the few adherent cells on low pMHC-densities may only have been in contact with a defective pattern, dirt or unusual protein accumulations. In any case, it was obvious that the spreading behavior of cells crucially depended on the particle distance: it was observed that many cells spread on substrates with low distance-spacing while only a significantly reduced number (close to zero) of adherent cells could be observed on substrates with higher distance-

spacing. The fact that the fraction of adhesive cells reached its maximum at 60% adhesion may reflect that only 60% of viable cells are competent to adhere. This is common in primary cell cultures as some of the viable cells are in the process of dying. Additionally, at a certain time point there is always a fraction of cells, which has already been adherent or will adhere at a future time point. On the low end there is typically a threshold below which no adhesion is observed, however there is still a small fraction of cells behaving aberrantly. These cells might have just adhered non-specifically or have found pattern defects as described above. However, the chosen method to quantify this experimental observation is a suitable way to translate this observation into numbers. This information in combination with the IL-2 data becomes very significant as the IL-2 secretion results correlate well with the cellular spreading data.

Quantification of IL-2 secretion: The reason why we chose to use the index of activation, thus a normalized value instead of absolute IL-2 values is because of the significant variability in each experiment, depending on factors such as cell densities that can be slightly different, proteins that may be less functional and most importantly, because living cells can behave differently depending on the cell batch used. Hence, the absolute values of IL-2 secretion can differ significantly (up to a factor 2 in this study) even under the same conditions. This difference is not due to the different surfaces used but to the circumstances described above. In order to eliminate this variability effect in a statistical assessment every type of surface would have to be included in each individual experiment. This, however, was not possible due to the large number of different surface parameters tested. Therefore, an alternative to eliminate the effect of differently behaving cell batches (or other unspecified effects) is to perform normalization. Therefore each

absolute IL-2 concentration value was compared to a control value, which in this study consisted of the amount of IL-2 that cells secreted when cultured on entirely coated pMHC surfaces (positive control surfaces). Thus, each experiment performed in included at least two positive control surfaces whose average IL-2 value was set as standard value 1.

Error determination for spacing and densities:

The distances *d* between Au nanoparticles and their deviations were determined using a custom-made plug-in for ImageJ, which calculated the average distance by comparing each pattern with an ideal hexagonal pattern. Here we provide the deviation for the single value but not for the mean value, as the latter can be made arbitrarily small since it depends on N (the higher the N, the smaller the error), which in this case corresponds to the number of particles taken into account. This number can be chosen to be very high therefore making the standard error of the mean very small. However, we found it reasonable to provide deviations of single values (for micrometer sized areas) as the cell senses single particle spacing or at least only averages within a restricted micrometer-sized area. The particle densities were calculated using the following equation:

$$\varrho = \frac{2}{\sqrt{3}} \times \frac{1}{d^2}, [\varrho] = number\ of\ particles/\mu m^2$$

with the deviation $s_\varrho = \frac{4\,\sigma_d}{\sqrt{3}} \times \frac{1}{d^3}, [s_\varrho] = number\ of\ particles/\mu m^2$

when σ_d is the deviation of the distance d.

It may seem strange that the absolute error bars for high densities are much higher than for low densities. This difference is not due to a specific pattern limitation but to the following: (i) the absolute values of densities, which for small distances are significantly higher (the relative deviations are not as high) and also to (ii) the Gaussian error propagation, which increases the relative error of densities in comparison to the relative errors of spacings. Since d is part of the equation for s_p with the power to three in the denominator the relative errors increase, in comparison to the relative errors of the distance. For example, for small distances approximately (34 ± 5) nm leads to a density of (1000 ± 300) particles/ μm^2 (30% relative deviation), while a distance of (276 ± 27) nm leads to a density of (15 ± 3) particles/ μm^2 (20 % relative deviation). When displayed in a graph as the one included in this manuscript, it can be seen that pattern deviation for high densities is much larger which is only true for the absolute value but not for relative deviations.

Determination of pMHC molecules per particle: The bulk fluorescence intensity measurements that were applied to determine to bound molecules per particle was, to the best of our knowledge, the most suitable to obtain statistical relevant values. 800 values out of 8 samples (2 chambers each) were determine in order to gather good statistics as it was observed that the number of bound molecules depends on several parameters: obvious ones like size of particles but also non-expected ones like incubation time, washing steps and time. Therefore, we followed a strict functionalization protocol for cell experiments and applied exactly the same procedural steps for the microscopy analysis.

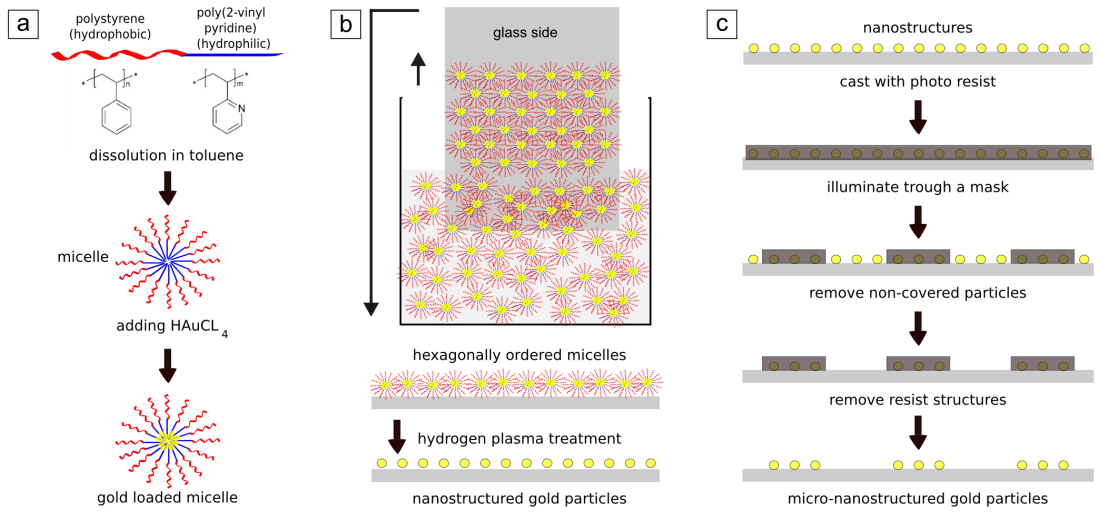

Figure S1: Schematic representation of the substrate fabrication steps: a) Au-loaded micelle formation process within a non-polar solvent; b) Formation of quasi-hexagonal nanopatterned Au particles on solid substrates; c) Fabrication of micro-nanostructured Au particles on solid substrates.

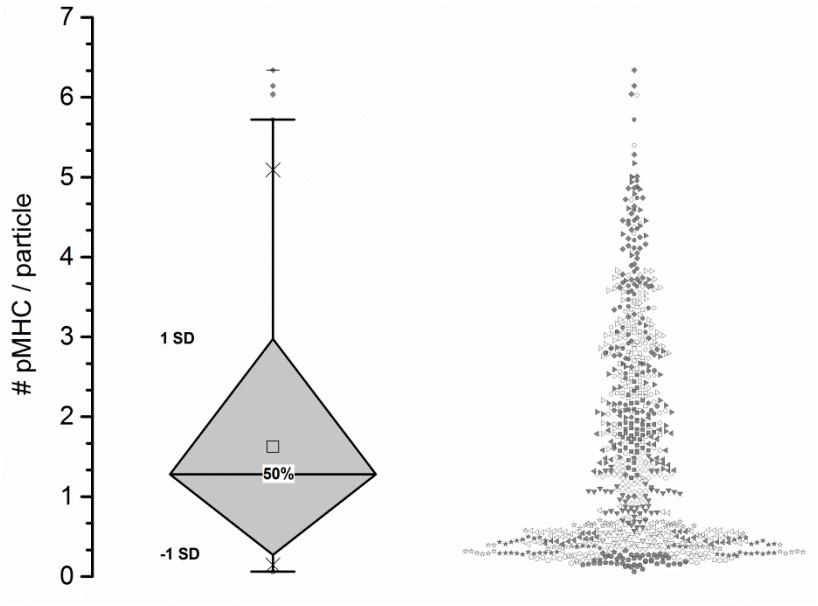

Figure S2: Occupation rate of pMHC molecules per Au particle for surfaces with distances between 100-150 nm (for each evaluated surface the distance was determined

312 individually). Symbols represent data points for the different surfaces. Same symbols
313 filled and non-filled represent data points from the same surface but correspond to
314 different chambers.